

1 **Carbohydrate Polymers, Original full-length research papers**

2

3 **Mineralization of hydroxyapatite upon a unique xanthan**
4 **gum hydrogel by an alternate soaking process**

5 Hironori Izawa^{a,*}, Shoji Nishino^a, Hiroyuki Maeda^a, Kohei Morita^a, Shinsuke Ifuku^a, Minoru
6 Morimoto^a, Hiroyuki Saimoto^a, Jun-ichi Kadokawa^b

7 ^aGraduate School of Engineering, Tottori University, 4-101 Koyama-Minami, Tottori 680-
8 8550, Japan.

9 ^bGraduate School of Science and Engineering, Kagoshima University, 1-21-40 Korimoto,
10 Kagoshima 890-0065, Japan.

11

12 *Corresponding to: Hironori Izawa.

13 Postal Address: Department of Science and Biotechnology, Graduate School of Engineering,
14 Tottori University, 4-101 Koyama-Minami, Tottori 680-8550, Japan.

15 Phone: +81-857-31-5813. Fax: +81-857-31-5813. E-mail: h-izawa@chem.tottori-u.ac.jp

16

17

1 **Abstract**

2 We previously reported a xanthan gum (Xan) hydrogel showing excellent mechanical
3 properties. Mineralization of hydroxyapatite (Hap) upon the Xan hydrogel would provide a
4 unique biomaterial applicable for bone tissue engineering. Here we show the mineralization of
5 Hap upon the Xan hydrogel by means of an alternate soaking process. Hap was gradually
6 grown upon the Xan-matrix surface with increasing number of soaking cycles due to the ionic
7 interactions between calcium cations and carboxyl groups. Interestingly, the mineralization
8 induced a micro-structure change in the gel-matrix from a layered structure to a porous
9 structure. The mechanical properties of the resulting Hap-Xan composite hydrogels were
10 further investigated by a tensile test, where the Hap-Xan composite hydrogel with an
11 appropriate amount of Hap (Xan/Hap = 2.7) was capable of approximately 370 % elongation.

12

13 **Key Word:** Xanthan gum, Hydroxyapatite, Alternate soaking process, Inorganic-organic
14 composite hydrogel, Mineralization

15

16 **1. Introduction**

17 Biom mineralization is a widespread phenomenon in nature leading to the formation of a
18 variety of solid inorganic structures by living organisms (Arias & Fernandez, 2008), in which
19 finely scaled and highly controlled inorganic precipitates are generated in organic matrixes
20 through self-assembled bottom-up processes under mild conditions (Calvert & Rieke, 1996).
21 These biologically produced biominerals are inorganic-organic hybrid composites showing
22 interesting properties, including controlled hierarchical structures and remodeling or repair
23 mechanisms that remain to be developed into a practical engineering process (Dujardin &
24 Mann, 2002; Heuer et al., 1992; Mann, 2000). Thus, biomimetic mineralization has been
25 emerging as an active area of recent research for the design of new materials and devices in
26 various fields (Colfen, 2007).

1 Hydroxyapatite (Hap) ($\text{Ca}_{10}(\text{PO}_4)_6(\text{OH})_2$) is the inorganic component of hard tissues of
2 vertebrate. Hap exhibits excellent biocompatibility with various kinds of cells and tissues
3 (Okada & Furuzono, 2012). The Hap-polymer composite, mimicking the composition and
4 structure of mineralized tissues, provides excellent mechanical properties in addition to
5 favorable biological properties, making it an ideal candidate for tissue engineering as well as
6 orthopedic and dental applications (Sun, Zhou & Lee, 2011). Anionic polysaccharides such as
7 alginate, hyaluronic acid, and chondroitin sulfate are potential optimal templates for the
8 mineralization of Hap because their anionic surface can bind Ca^{2+} ions and can control crystal
9 nucleation and growth by lowering the interfacial energy between the crystal and the surface
10 (Arias & Fernandez, 2008). Therefore, various Hap-composited materials have been prepared
11 by using anionic polysaccharides for biomedical applications, including bone tissue
12 engineering (Chen, Ushida & Tateishi, 2002; Du, Song, Cui, Yang & Li, 2011; Green et al.,
13 2005; Shi, Zhang, Qi & Cao, 2012; Shi, Zhang, Yang & Tang, 2009; Zhong & Chu, 2012).

14 Xanthan gum (Xan), which is a water-soluble anionic polysaccharide produced by
15 *Xanthomonas campestris*, is a useful food hydrocolloid (Jansson, Kenne & Lindberg, 1975). It
16 has a cellulose main-chain ((1 / 4)- β -glucan) with trisaccharide anionic sidechains attached to
17 alternate glucose units in the main-chain (Melton, Mindt, Rees & Sanderson, 1976). Xan has
18 been widely used in a broad range of industries as a rheological control agent in aqueous
19 systems and as a stabilizer for emulsions and suspensions (Rosalam & England, 2006). In
20 general, an aqueous dispersion of Xan exhibits only weak gel-like behavior in the presence of
21 a sufficient amount of inorganic salt because it is a micro-gel with a double-helix
22 conformation (Alistair, Glyn & Peter, 2006). We have discovered, however, that Xan can be
23 converted to a Xan hydrogel with excellent mechanical properties by means of a gelation
24 process with 1-butyl-3-methylimidazolium chloride (BMIMCl) (Fig. 1) (Izawa & Kadokawa,
25 2010; Izawa, Kaneko & Kadokawa, 2009). When Xan is heated at 100 °C in BMIMCl, the
26 double-helix conformation of Xan is disentangled, resulting in dissolution. Subsequent

1 cooling of the Xan/BMIMCl solution to room temperature then induces gelation. The
2 Xan/BMIMCl gel was soaked in a large volume of pure water to create the Xan hydrogel, in
3 which the double-helix conformation of Xan was restored in response to the high ionic
4 strength (Camesano & Wilkinson, 2001). Although the chemical structure of Xan did not
5 change during the gelling process, the Xan hydrogel was surprisingly capable of
6 approximately 500 % strain in the tensile test (Izawa & Kadokawa, 2010). Such a
7 polysaccharide hydrogel having both a tough and elastic nature is quite rare. In addition, the
8 Xan hydrogel can potentially serve as an organic template for biomimetic mineralization
9 because Xan has carboxyl groups in its residue. The mineralization of Hap upon a Xan-matrix
10 surface would provide a high performance Hap-composited hydrogel applicable to bone tissue
11 engineering. Here we show the mineralization of Hap upon the Xan hydrogel. The Xan
12 hydrogel prepared by using BMIMCl was subjected to an alternate soaking process (Taguchi,
13 Kishida & Akashi, 1998). The resulting Hap-Xan composite hydrogel was evaluated by
14 infrared spectroscopy (IR), X-ray diffraction spectroscopy (XRD), scanning electron
15 microscopy (SEM), and energy-dispersive X-ray spectrometry (EDX) analyses. The
16 mechanical properties of the Hap-Xan composite hydrogel were further investigated by tensile
17 test.

18

19 **2. Experiments**

20 **2.1. Materials**

21 BMIMCl was purchased from Sigma-Aldrich Japan (Tokyo, Japan). Xan (viscosity;
22 1785 cps, 1 wt% solution in 1 wt% KCl aq., 20 °C) was purchased from Tokyo Chemical
23 Industry Co., Ltd. (Tokyo, Japan). Commercial products of Xan have a moisture content of ca.
24 11 % and an ash content of 6-9 % (Alistair, Glyn & Peter, 2006). The molecular weights of
25 the Xan samples are generally $2-50 \times 10^6$ Da (Alistair, Glyn & Peter, 2006). Other reagents
26 were used as commercial grade without further purification.

1
2
3
4
5
6
7
8
9
10
11
12
13
14
15
16
17
18
19
20
21
22
23
24
25
26

2.2. Preparation of the Xan hydrogel

Xan (0.10 g, i.e., 9.1 wt%) was added to BMIMCl (1.00 g) and stirred for 3 min at 100 °C to create a homogeneous solution. After the solution was continuously heated at 100 °C for 12 h without stirring to completely dissolve Xan, it was kept at room temperature for 30 min to give a xanthan/BMIMCl gel. The Xan/BMIMCl gel was compressed at 100 °C for 10 min by hot-pressing with a 0.5 mm thick spacer to create a film gel. The Xan/BMIMCl gel film was soaked in pure water (100 mL) at 5 °C for 12 h. The Xan hydrogel was picked up from the water and was subsequently soaked in 0.5 M CaCl₂ aqueous solution (10 mL) at 5 °C for 12 h, followed by soaking in pure water (100 mL) for 12 h at 5 °C.

2.3. Preparation of the Hap-Xan composite hydrogel

Conditions for the alternate soaking process were utilized as reported previously (Ngiam, Liao, Patil, Cheng, Chan & Ramakrishna, 2009). The Xan hydrogel was first soaked in 0.3 M Na₂HPO₄ aqueous solution (10 mL) at 37 °C for 1 h, followed by soaking in pure water (100 mL) for 1 h at room temperature. Next, the Xan hydrogel was soaked in 0.5 M CaCl₂ aqueous solution (10 mL) at 37 °C for 1 h, followed by soaking in pure water (100 mL) for 1 h at room temperature. This alternate soaking cycle was repeated for 5 or 10 cycles.

2.4. Measurements

Infrared spectra of the samples were recorded with an FT-IR spectrophotometer (Spectrum 65, Perkin-Elmer Japan Co., Ltd., Japan) equipped with an ATR attachment. X-ray diffraction profiles were obtained with Ni-filtered CuK α from an X-ray generator (Ultima IV, Rigaku, Japan) operating at 40 kV and 30 mA. The diffraction profile was detected using an X-ray goniometer scanning from 10° to 60°. For field emission scanning electron microscopic (FE-SEM) observation, the sample was coated with an approximately 2 nm layer of Pt by an

1 ion sputter coater and observed by FE-SEM (JSM-6700F; JEOL, Ltd., Japan), equipped with
2 energy dispersive X-ray microanalyzer (JED-2200, JEOL Ltd., Japan), operating at 2.0 kV.
3 EDX spectrum was measured without Pt-coating. Tensile strengths and Young's moduli were
4 measured by a universal testing instrument (AG-10KNX, Shimadzu, Japan) for samples 50
5 mm long and 10 mm wide at a cross head speed of 1 mm min⁻¹ with a gage length of 30 mm.

6

7 **3. Results and Discussion**

8 **3.1 Preparation of the Hap-Xan composite hydrogel**

9 The Xan/BMIMCl gel (9.1 wt%) was prepared by the previously reported method (Fig.
10 2a) (Izawa & Kadokawa, 2010). When the Xan hydrogel was subjected to the alternate
11 soaking process, the Xan hydrogel was allowed to reach equilibrium in the solutions. Film
12 shape enabled equilibration with a shorter soaking time because of the larger contact area to
13 water. The Xan/BMIMCl gel was therefore processed into a gel film (ca 0.5 mm thick) by
14 hot-pressing. The Xan/BMIMCl film gel was subsequently converted to a Xan hydrogel by
15 soaking in a large volume of pure water. The hydrogel was ion-exchanged to Ca²⁺. Residual
16 salt in the Xan hydrogel was removed by soaking in a large volume of pure water.

17 Next, mineralization of Hap upon the Xan hydrogel by the alternate soaking process
18 was investigated (Fig. 2b). The Xan hydrogel gradually turned white with soaking cycles of
19 increasing length due to the mineralization of Hap. Interestingly, the weights of the hydrogels
20 were reversibly changed during the alternate soaking process (Fig. 2c). When the hydrogel
21 was soaked in pure water, it immediately swelled, whereas the swollen volume after soaking
22 in CaCl₂ aqueous solution was much smaller than that after soaking in Na₂HPO₄ aqueous
23 solution due to the ionic crosslinking of Ca²⁺. In contrast, the swollen hydrogel immediately
24 shrunk in Na₂HPO₄ and CaCl₂ aqueous solution. This behavior is similar to previously
25 reported swelling-shrinking behavior of the Xan hydrogel (Izawa & Kadokawa, 2010). As
26 described in the introduction, the conformation of Xan is reversibly changed from a double-

1 helix to a single chain in response to a high or low ionic strength (Camesano & Wilkinson,
2 2001), which caused reversible swelling-shrinking behavior of the Xan hydrogel (Izawa &
3 Kadokawa, 2010). In addition, the weight of the initial Xan hydrogel (Ca^{2+} form) after
4 soaking in pure water in the first cycle increased to ca 1.5 times after 10 cycles. It is thought
5 that this increase was caused by a reduction in the quantity of the double-helix part in the
6 Xan-matrix as described hereinafter.

7

8 **3.2 Analysis of the Hap-Xan composite hydrogel**

9 IR and XRD analyses of lyophilized-composite hydrogels were investigated to
10 confirm the production of Hap. Fig. 3a shows the IR spectra of the lyophilized-Xan hydrogel
11 (blank) and the Hap-Xan composite hydrogel obtained by 5- or 10-cycles (a so-called 5- or
12 10-cycle gel, respectively). The absorption peaks due to PO_4^{3-} for Hap are shown at 570 cm^{-1} ,
13 603 cm^{-1} , 962 cm^{-1} , and 1045 cm^{-1} (Tas, 2000). Although the absorption peaks at 962 cm^{-1}
14 and 1045 cm^{-1} were overlapped with those of Xan, the absorption peaks at 570 cm^{-1} and 603
15 cm^{-1} (pointed by arrows) were clearly observed in the 5- and 10-cycle gels, which is
16 suggestive of the production of Hap. Fig. 3b shows XRD patterns of blank and 5- and 10-
17 cycle gels. In the spectrum of the blank, the broad diffraction peak corresponding to the
18 double-helix conformation of Xan was only observed at around 20° (Alistair, Glyn & Peter,
19 2006; Millane & Narasaiah, 1990; Moorhouse, Walkinshaw & Arnott, 1977). In contrast, in
20 those of the 5- and 10-cycle gels, distinct diffraction peaks were observed at 25.9° , 28.3° ,
21 33.5° , 38.9° , 46.3° , 49.3° , and 53.2° (pointed by arrows) in agreement with the reported
22 diffraction peaks for Hap (Tas, 2000), indicating production of Hap upon the Xan hydrogel.
23 On the other hand, the broad diffraction peak due to the double-helix conformation of Xan
24 gradually disappeared with increases in the number of soaking cycles, suggesting that the
25 mineralization of Hap upon the Xan hydrogel involves a reduction of the double-helix part of
26 the Xan-matrix. This result is consistent with the aforementioned swelling behavior being

1 dependent on the soaking cycles because the decreasing quantity of the double-helix part
2 presenting as a junction zone allows water absorption. The reason for the reduction in the
3 double-helix part is thought to be that Hap-deposited Xan single chains cannot restore the
4 double-helix conformation because of the hindrance of Hap (Fig. 3c).

5 Fig. 4 shows SEM images of the cross-sections of the lyophilized hydrogels. A multi-
6 layered structure was observed in the blank (Fig. 4a), whereas the micro-structure was
7 dramatically changed after mineralization. In the 5-cycle gel, a porous structure composed of
8 nano-flakes was observed (Fig. 4b). The nano-flakes were grown by further soaking up to 10
9 cycles (Fig. 4c). To confirm the composition of the nano-flakes, EDX analysis was
10 investigated (Fig. 4f). In the EDX spectrum, the presence of Ca, P, and O was observed,
11 suggesting that the nano-flakes were definitely Hap. In addition, the Ca/P atomic ratio was
12 estimated to be 1.65, which was slightly lower than the theoretical Ca/P atomic ratio of Hap
13 ($\text{Ca}_{10}(\text{PO}_4)_6(\text{OH})_2$; 1.67). The chemical formula estimated from the Ca/P ratio was
14 ($\text{Ca}_{9.9}(\text{HPO}_4)_{0.1}(\text{PO}_4)_{5.9}(\text{OH})_2$), which was classified as calcium-deficient Hap (Okada &
15 Furuzono, 2012). Note that SEM images of the Hap-Xan composite hydrogel surface are
16 almost the same as the aforementioned cross-sectional images, indicating that the Hap-Xan
17 composite hydrogels were completely equilibrated during the alternate soaking process.

18 Although Hap was observed in the SEM analysis of the 5- and 10-cycle gels, the Xan-
19 matrix was not recognized. We supposed that the Xan-matrix was completely hidden behind
20 the Hap-flakes. SEM analysis of a 1-cycle gel with a Xan/Hap ratio of 15.4 was therefore
21 carried out (Fig. 4d). Interestingly, a structure change from a layered to a porous structure was
22 observed at this stage, indicating that the micro-structure change was induced even by the
23 slight nucleation and was caused by the morphology change of the Xan-matrix due to
24 mineralization. SEM analysis of the swelling-gel (Na^+ form) obtained after soaking in pure
25 water during the 10th cycle was further investigated (Fig. 4e), with nano-fibrils (ca 10 nm) of
26 Xan being observed on the space between the Hap-flakes. This result suggests that the Xan-

1 matrix was completely adhering to the Hap-surface through ionic interactions in the case of
2 the Ca^{2+} form, and it therefore was not observed in the SEM analysis.

3 The Hap contents of the 5- and 10-cycle gels were estimated by the difference in the
4 weight of the dried-blank and dried-5- and 10-cycle gels, respectively. The Hap contents of
5 the 5- and 10-cycle gels were 1.9 % and 4.8 %, respectively, which was clearly dependent on
6 the number of soaking cycles. This result is consistent with the results in the SEM analysis
7 where the Hap amount of the 10-cycle gel was obviously greater than that of the 5-cycle gel.
8 The water content was estimated by the difference in the weight of the hydrogel and that of
9 the dried-material. The water contents of the 5- and 10-cycle gels were 93.0 % and 91.2 %,
10 respectively, which were higher than that of the blank (89.9 %). The result is probably due to
11 the decreased quantity of the double-helix part in the Xan-matrix, as mentioned above.

12

13 **3.3 Mechanical properties of the Hap-Xan composite hydrogel**

14 Fig. 5a shows the stress-strain curves of the blank and 5- and 10-cycle gels under
15 tensile mode. The fracture stress and strain of the blank were 99.8 kPa and 471.3 %,
16 respectively. These values were similar to those reported previously (Izawa, Kaneko &
17 Kadokawa, 2009). Unfortunately, however, those of the 5- and 10-cycle gels were reduced to
18 68.9 kPa and 376.4 % and 59.8 kPa and 204.8 %, respectively. This reduction in mechanical
19 strength was probably caused by the decreased quantity of the double-helix part, as the
20 presence of a junction point generally enhances the gel strength (Kuo & Ma, 2008). On the
21 other hand, Young's modulus was increased with increasing amounts of Hap, with values for
22 the 5- and 10-cycle gels being 1.1 or 1.6 times that of the blank, respectively (Fig. 5b). Thus,
23 it is supposed that the fracture stress of the Hap-Xan composite hydrogel depends on the
24 quantity of the double-helix part of the Xan-matrix. In contrast, increasing amounts of Hap
25 slightly enhance the Young's modulus. It should be noted that although mechanical strength

1 was reduced by the mineralization as compared to the blank, the strength remained high, as
2 shown in Fig. 5c. Typical polysaccharide gels don't show such elasticity.

3

4 **4. Conclusion**

5 In this study, Hap was successfully mineralized upon the Xan hydrogel by the alternate
6 soaking process, where the Xan-matrix worked as a scaffold due to the presence of carboxyl
7 groups. The content of Hap in the Hap-Xan composite hydrogel was clearly dependent on the
8 soaking cycles. Interestingly, the mineralization of Hap induced a micro-structure change of
9 the Xan hydrogel from a layered structure to a porous structure. In addition, the double-helix
10 part of the Xan hydrogel decreased with increases in the number of soaking cycles because
11 the produced-Hap avoided restoration of the double-helix conformation. Furthermore, the
12 mechanical properties of the Hap-Xan composite hydrogel were investigated by the tensile
13 test. Although the mechanical strength of the Hap-Xan composite hydrogel was reduced with
14 increasing the number of soaking cycles, the mechanical strength remained high even after 5
15 or 10 cycles, which allowed for approximately 380 and 200 % elongation, respectively. There
16 have previously been no reports of such elastic Hap-composited hydrogels. This Hap-Xan
17 composite hydrogel showing unique mechanical properties would be a powerful tool for a
18 scaffold material for bone tissue engineering (Chen, Ushida & Tateishi, 2002). In addition, the
19 Hap-Xan composite material is applicable for use as a force-responsive material in
20 mechanobiochemistry (Brantley, Bailey, Wiggins, Keatinge-Clay & Bielawski, 2013) to
21 provide new scientific knowledge.

22

23 **Acknowledgements**

24 This work was in part supported by the *Tottori Prefecture Environment and Academic*
25 *Promotion Project.*

26

1 **References**

- 2 Alistair, M. S., Glyn, O. P., & Peter, A. W. (Eds.). (2006). *Food polysaccharides and their*
3 *applications*. London: CRC press.
- 4 Arias, J. L., & Fernandez, M. S. (2008). Polysaccharides and Proteoglycans in Calcium
5 Carbonate-based Biomineralization. *Chemical Reviews*, 108(11), 4475-4482.
- 6 Brantley, J. N., Bailey, C. B., Wiggins, K. M., Keatinge-Clay, A. T., & Bielawski, C. W.
7 (2013). Mechanobiochemistry: harnessing biomacromolecules for force-responsive materials.
8 *Polymer Chemistry*, 4, 3916-3928.
- 9 Calvert, P., & Rieke, P. (1996). Biomimetic mineralization in and on polymers. *Chemistry of*
10 *Materials*, 8(8), 1715-1727.
- 11 Camesano, T. A., & Wilkinson, K. J. (2001). Single molecule study of xanthan conformation
12 using atomic force microscopy. *Biomacromolecules*, 2(4), 1184-1191.
- 13 Chen, G. P., Ushida, T., & Tateishi, T. (2002). Scaffold design for tissue engineering.
14 *Macromolecular Bioscience*, 2(2), 67-77.
- 15 Colfen, H. (2007). Bio-inspired mineralization using hydrophilic polymers. *Topics in Current*
16 *Chemistry*, 271, 1-77.
- 17 Du, M. C., Song, W. X., Cui, Y., Yang, Y., & Li, J. B. (2011). Fabrication and biological
18 application of nano-hydroxyapatite (nHA)/alginate (ALG) hydrogel as scaffolds. *Journal of*
19 *Materials Chemistry*, 21(7), 2228-2236.
- 20 Dujardin, E., & Mann, S. (2002). Bio-inspired materials chemistry. *Advanced Materials*,
21 14(11), 775-788.
- 22 Green, D. W., Leveque, I., Walsh, D., Howard, D., Yang, X. B., Partridge, K., Mann, S., &
23 Oreffo, R. O. C. (2005). Biomineralized polysaccharide capsules for encapsulation,
24 organization, and delivery of human cell types and growth factors. *Advanced Functional*
25 *Materials*, 15(6), 917-923.
- 26 Heuer, A. H., Fink, D. J., Laraia, V. J., Arias, J. L., Calvert, P. D., Kendall, K., Messing, G. L.,
27 Blackwell, J., Rieke, P. C., Thompson, D. H., Wheeler, A. P., Veis, A., & Caplan, A. I. (1992).
28 Innovative Materials Processing Strategies - a Biomimetic Approach. *Science*, 255(5048),
29 1098-1105.
- 30 Izawa, H., & Kadokawa, J. (2010). Preparation and characterizations of functional ionic
31 liquid-gel and hydrogel materials of xanthan gum. *Journal of Materials Chemistry*, 20(25),
32 5235-5241.
- 33 Izawa, H., Kaneko, Y., & Kadokawa, J. (2009). Unique gel of xanthan gum with ionic liquid
34 and its conversion into high performance hydrogel. *Journal of Materials Chemistry*, 19(38),
35 6969-6972.
- 36 Jansson, P. E., Kenne, L., & Lindberg, B. (1975). Structure of Extracellular Polysaccharide
37 from *Xanthomonas-Campestris*. *Carbohydrate Research*, 45(Dec), 275-282.
- 38 Kuo, C. K., & Ma, P. X. (2008). Maintaining dimensions and mechanical properties of
39 ionically crosslinked alginate hydrogel scaffolds in vitro. *Journal of Biomedical Materials*
40 *Research Part A*, 84A(4), 899-907.
- 41 Mann, S. (2000). The chemistry of form. *Angewandte Chemie-International Edition*, 39(19),
42 3393-3406.
- 43 Melton, L. D., Mindt, L., Rees, D. A., & Sanderson, G. R. (1976). Covalent Structure of
44 Extracellular Polysaccharide from *Xanthomonas-Campestris* - Evidence from Partial
45 Hydrolysis Studies. *Carbohydrate Research*, 46(2), 245-257.
- 46 Millane, R. P., & Narasaiah, T. V. (1990). X-Ray Fiber Diffraction Studies of a Variant of
47 Xanthan Gum in Which the Sidechain Terminal Mannose Unit Is Absent. *Carbohydrate*
48 *Polymers*, 12(3), 315-321.
- 49 Moorhouse, R., Walkinshaw, M. D., & Arnott, S. (1977). Xanthan Gum—Molecular
50 Conformation and Interactions. (pp. 90-102). Washington DC.

1 Ngiam, M., Liao, S. S., Patil, A. J., Cheng, Z. Y., Chan, C. K., & Ramakrishna, S. (2009). The
2 fabrication of nano-hydroxyapatite on PLGA and PLGA/collagen nanofibrous composite
3 scaffolds and their effects in osteoblastic behavior for bone tissue engineering. *Bone*, 45(1), 4-
4 16.

5 Okada, M., & Furuzono, T. (2012). Hydroxylapatite nanoparticles: fabrication methods and
6 medical applications. *Science and Technology of Advanced Materials*, 13(6).

7 Rosalam, S., & England, R. (2006). Review of xanthan gum production from unmodified
8 starches by *Xanthomonas compestris* sp. *Enzyme and Microbial Technology*, 39(2), 197-207.

9 Shi, J., Zhang, Z. Z., Qi, W. Y., & Cao, S. K. (2012). Hydrophobically modified
10 biomaterialized polysaccharide alginate membrane for sustained smart drug delivery.
11 *International Journal of Biological Macromolecules*, 50(3), 747-753.

12 Shi, Y., Zhang, Y. H., Yang, W. L., & Tang, Y. (2009). Multiradiate calcium phosphate
13 patterns derived from a gradating polysaccharide-acidic protein system. *Chemical*
14 *Communications*(4), 442-444.

15 Sun, F., Zhou, H., & Lee, J. (2011). Various preparation methods of highly porous
16 hydroxyapatite/polymer nanoscale biocomposites for bone regeneration. *Acta Biomaterialia*,
17 7(11), 3813-3828.

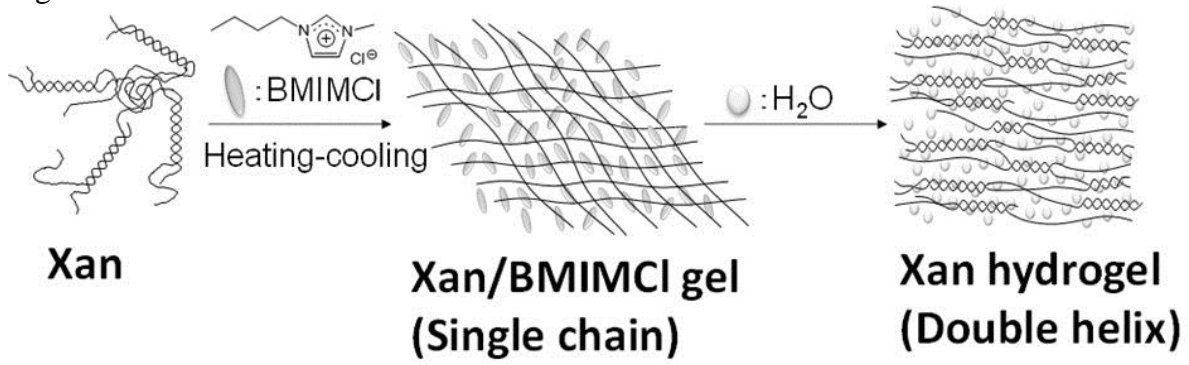
18 Taguchi, T., Kishida, A., & Akashi, M. (1998). Hydroxyapatite formation on/in poly(vinyl
19 alcohol) hydrogel matrices using a novel alternate soaking process. *Chemistry Letters*(8), 711-
20 712.

21 Tas, A. C. (2000). Synthesis of biomimetic Ca-hydroxyapatite powders at 37 degrees C in
22 synthetic body fluids. *Biomaterials*, 21(14), 1429-1438.

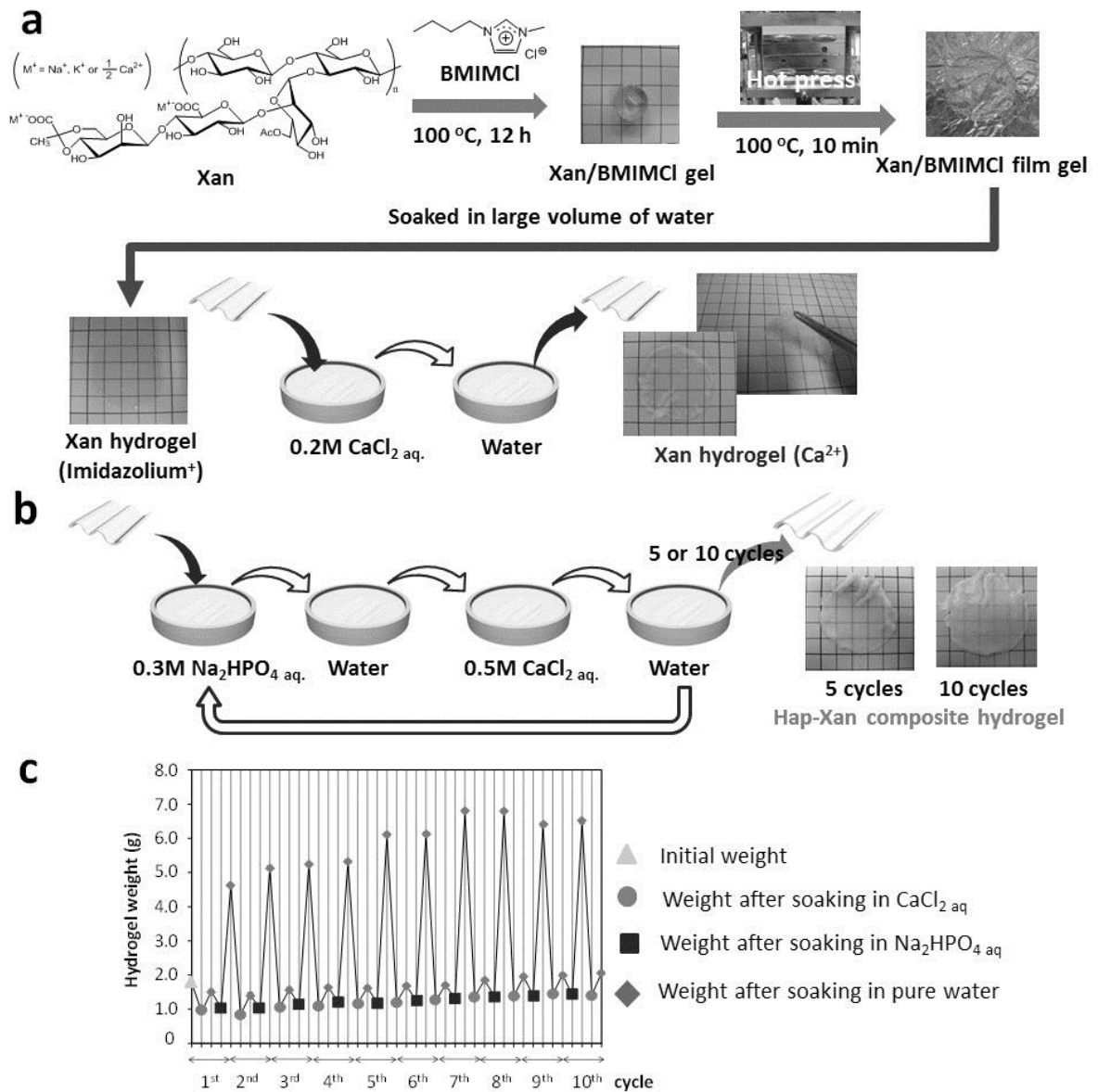
23 Zhong, C., & Chu, C. C. (2012). Biomimetic mineralization of acid polysaccharide-based
24 hydrogels: towards porous 3-dimensional bone-like biocomposites. *Journal of Materials*
25 *Chemistry*, 22(13), 6080-6087.

26
27

1 Fig. 1

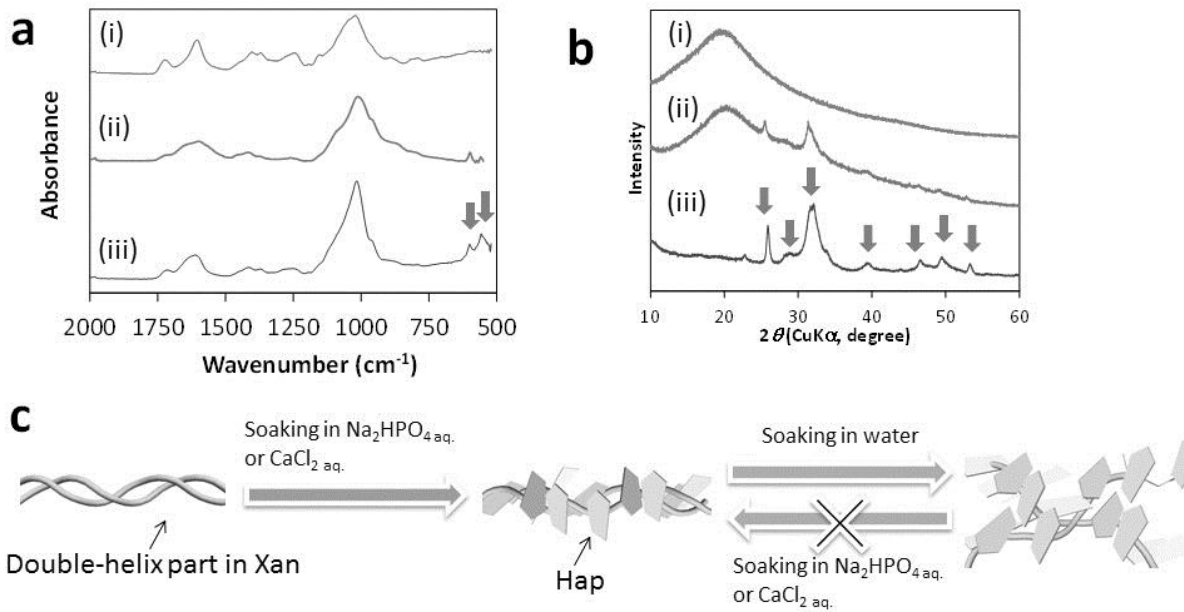


2
3 Fig. 2

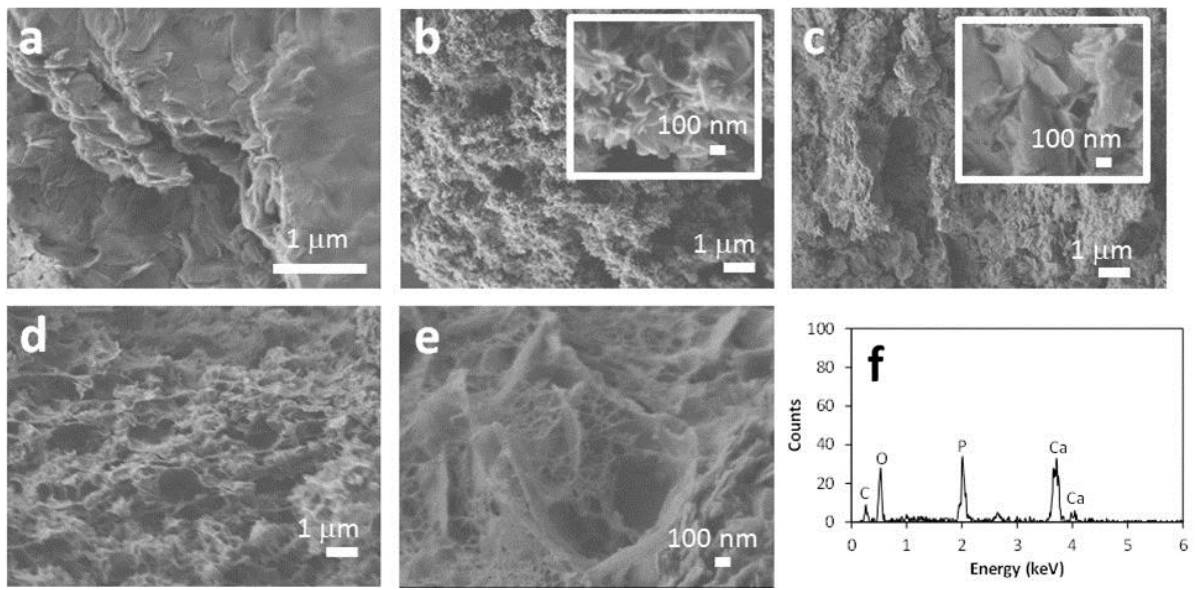


4
5
6

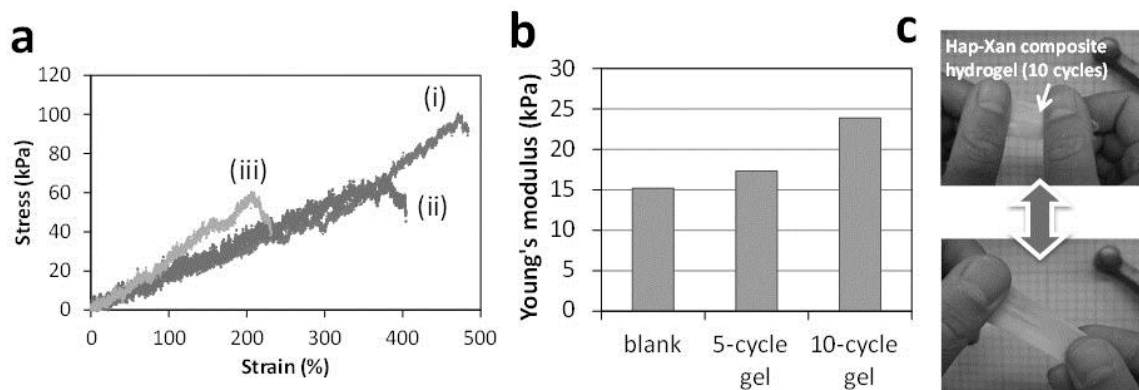
1
2 Fig. 3



3
4
5 Fig. 4



6
7
8 Fig. 5



1
2

3 **Figure Captions**

4 **Fig. 1.** Preparation of the Xan hydrogel with BMIMCl.

5 **Fig. 2.** Preparation of the Hap-Xan composite hydrogel by the alternate soaking process.

6 Schematic image of preparation of the Xan hydrogel (Ca^{2+}) (a) and the alternate soaking
7 process (b). Hydrogel weight during the alternate soaking process (c).

8 **Fig. 3.** IR spectra of the blank (i) and 5- (ii) and 10-cycle gels (iii) (a) and XRD patterns of
9 the blank (i), 5- (ii) and 10-cycle gels (iii) (b). Plausible mechanism for reduction of the
10 double-helix part (c).

11 **Fig. 4.** SEM images of blank (a), 5-cycle gel (b), 10-cycle gel (c), 1-cycle gel (d), and the
12 swelled-10-cycle gel (e). EDX spectrum of the 5-cycle gel (f).

13 **Fig. 5.** Stress-strain curves (a) and Young's moduli (b) of blank (i), 5- (ii) and 10-cycle gels
14 (iii). An image of the elongated-10 cycle gel (c).